



IAEA-FI-CN-69/EX1/4 (C1, C2)

## H-MODE REGIMES AND OBSERVATIONS OF CENTRAL TOROIDAL ROTATION IN ALCATOR C-MOD

M. GREENWALD, J. RICE, R. BOIVIN, P. BONOLI, R. BUDNY<sup>2</sup>, C. S. CHANG<sup>1</sup>, D. ERNST<sup>2</sup>, C. FIORE, J. GOETZ, R. GRANETZ, A. HUBBARD, I HUTCHINSON, J. IRBY, B. LABOMBARD, B. LIPSCHULTZ, E. MARMAR, D. MOSSESIAN, M. PORKOLAB, W. ROWAN<sup>4</sup>, J. SNIPES, G. SCHILLING<sup>2</sup>, Y. TAKASE<sup>5</sup>, J. TERRY, S. WOLFE, J. WEAVER<sup>3</sup>, B. WELCH<sup>3</sup>, S. WUKITCH

MIT - Plasma Science & Fusion Center

<sup>1</sup>New York University

<sup>2</sup>Princeton Plasma Physics Laboratory.

<sup>3</sup>University of Maryland

<sup>4</sup>University of Texas at Austin

<sup>5</sup>University of Tokyo

### Abstract

The Enhanced  $D_\alpha$  or EDA H-mode regime in Alcator C-Mod has been investigated and compared in detail to ELM-free plasmas. (In this paper, ELM-free will refer to discharges with no type I ELMs and with no sign of EDA, though technically, most EDA plasmas are ELM-free as well.) EDA discharges have only slightly lower energy confinement than comparable ELM-free ones, but show markedly reduced impurity confinement. Thus EDA discharges do not accumulate impurities and typically have a lower fraction of radiated power. EDA plasmas are seen to be more likely at low plasma current ( $q > 3.7 - 4$ ), for moderate plasma shaping, (0.35 - 0.55), and for high neutral pressures. No obvious trends were observed with input power or pressure ( $\beta$ ). In both H-mode regimes, and in ICRF heated L-modes, central impurity toroidal rotation has been deduced, from the Doppler shifts of argon x-ray lines. Rotation velocities up to  $1.3 \times 10^5$  m/s in the co-current direction have been observed in H-mode discharges that had no direct momentum input. There is a strong correlation between the increase in the central impurity rotation velocity and the increase in the plasma stored energy, induced by ICRF heating. In otherwise similar discharges with the same stored energy increase, plasmas with lower current rotate faster. The ion pressure gradient is an unimportant contributor to the central impurity rotation and the presence of a substantial core radial electric field is inferred during the ICRF pulse. An inward shift of ions induced by ICRF waves could give rise to a non-ambipolar electric field in the plasma core. Comparisons with a neo-classical ion orbit shift model show good agreement with the observations, both in magnitude, and in the scaling with plasma current.

### 1. Background

The observations presented here were obtained from the Alcator C-Mod tokamak, a compact (major radius  $R = 0.67$  m, minor radius  $a = 0.22$  m), high field device ( $2.6 < B_T < 7.9$  T) which has operated with plasma currents between 0.23 and 1.5 MA and average electron densities between 0.24 and  $5.9 \times 10^{20}/\text{m}^3$  (gas fueled). The standard shape for C-Mod plasmas has an elongation ( $\kappa$ ) between 1.55 and 1.75, lower triangularity ( $\delta_L$ ) near 0.5 and an upper triangularity ( $\delta_U$ ) near 0.3. Up to 3.5 MW of ICRF power at 80 MHz is available, from 2 dipole antennas, each with  $0, \pi$  phasing; the cases described here are all with H minority heating. Total input power can reach 4.5 MW. H-modes are obtained under a wide variety of conditions.

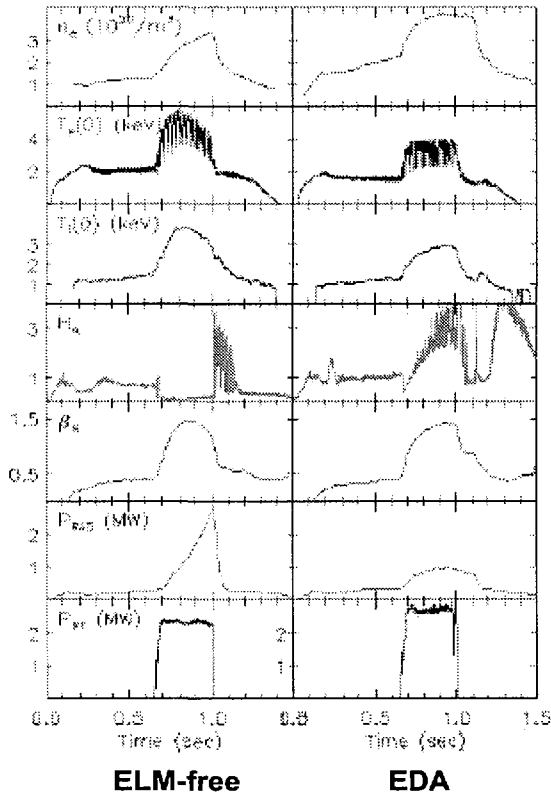


Fig 1. Characteristic traces from ELM-free and EDA H-modes. Note the difference in the  $H\alpha$  and  $P_{RAD}$  signals. The controlling difference between these shots is the target density, which is higher for EDA.

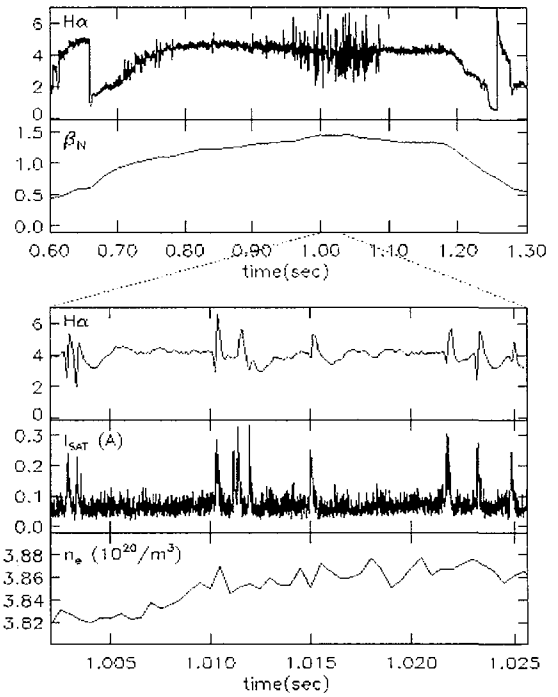


Fig 2. As  $\beta_N$  rises above 1.2-1.3 small ELMs appear on top of the EDA. Also shown on an expanded time scale is  $H\alpha$ , the ion saturation current from a divertor probe and the line averaged density. While some plasma exhaust is clearly visible on the probes, there is no measurable loss of particles from the plasma.

## 2. EDA and ELM-free H-modes

We have observed a promising H-mode regime, which can evolve out of ELM-free discharges and is characterized by good energy confinement, moderate particle confinement, and no type I ELMs. [1,2]. The edge temperature can reach 600-800 eV, well above the threshold for type III ELMs, and the pressure gradient in the transport barrier would seem to challenge MHD stability limits. We have named this regime EDA or Enhanced  $D_\alpha$  mode after its salient characteristic. Traces comparing typical ELM-free and EDA discharges are shown in figure 1. Unlike ELM-free discharges, which have long impurity confinement time and often end with a radiative collapse, this regime seems to have true steady-state potential. The EDA can last, without obvious change, for the duration of the RF heating pulse, about 10 energy confinement times. Unlike standard ELMy discharges, EDA plasmas show no intermittent loss of particles and energy. The peak heat loads associated with type I ELMs can reach unacceptable levels when extrapolated to reactor scale devices. In an EDA discharge, the edge gradients seem to be limited by a continuous process, rather than a periodic one.

EDA may be related to regimes seen on other devices, notably JET's Low Particle Confinement (LPC) H-mode[3] which was also obtained with ICRF heating. It also shares some characteristics with type II ELMs reported by DIII-D[4] and small ELMs seen on JT60-U when the plasma triangularity was increased[5]. In all of these cases, good energy confinement is combined with increased particle transport, leading to H-modes without impurity accumulation. The LPC mode lasted only about 1 second and type II ELMy discharges were also transient, with type I ELMs eventually returning. The occurrence of these regimes is consistent with the effects of plasma shaping which are described in more detail below; the disappearance of large ELMs is strongly correlated with

plasma triangularity. Unraveling the connection between EDA and other “small” ELM regimes is made somewhat confusing by the appearance of low amplitude ELMs on top of an EDA background. Shown in figure 2, these ELMs occur when  $\beta$  rises above a threshold roughly characterized by  $\beta_N \sim 1.2-1.3$ . It is possible that devices operating consistently above this level would never see a “pure” EDA.

In Alcator C-Mod, energy confinement enhancement relative to the ITER89 L-mode scaling is found to be, on average, 1.8 for EDA discharges and 2.1 for ELM-free. EDA confinement is about 15% higher than the ITER97 H-mode scaling for ELMy plasmas. The difference in confinement between the two regimes reflects the difference in their pedestal temperatures. In C-Mod, a simple offset-linear relation exists between edge temperature and global confinement[2]. This relation is consistent with marginal stability and critical gradient-length models of plasma transport. For discharges with radiated power more than 50% of the input power, confinement begins to decrease, approaching L-mode levels for radiated fractions over 0.9[2]. High neutral pressures are also associated with degraded confinement. Plasmas with midplane pressures greater than 0.2-0.3 mTorr (divertor pressures  $> 40$ mTorr) begin to show a drop in confinement, a trend which continues to the highest recorded pressures which were above 1 mTorr (divertor pressure  $\sim 150-200$  mTorr) where  $\tau_E$  is close to L-mode levels. The drop in confinement is continuous and even in the extreme cases, the discharges are clearly still in H-mode; discrete transitions can be seen on edge diagnostics when the plasma returns to L-mode. When comparing with global scaling laws, consideration is limited to discharges with radiated power fraction  $< 0.50$  and divertor neutral pressure  $< 40$  mTorr. Impurity particle confinement,  $\tau_i$ , in EDA plasmas is in the range 0.15-0.2 seconds, roughly  $2-3 \times \tau_E$ , unlike ELM-free plasmas where  $\tau_i > 0.5$  seconds. Analysis of impurity profile evolution shows higher diffusivity and a weaker pinch for EDA discharges than for ELM-free. In C-Mod, the density rise that accompanies the L/H transition is large enough to keep the plasma near the global power threshold even at the highest powers available. The data are all taken in the range  $P/P_{\text{THRESHOLD}} \sim 0.9-1.6$ , where  $P_{\text{THRESHOLD}}$  is taken to be proportional to density and evaluated in the fully developed H-mode. There is no obvious trend for discharges nearer the global threshold to have lower confinement.

The difference in pedestal temperature and impurity confinement in EDA may be the result of transport driven by enhanced levels of turbulence which have been observed in the edge of these plasmas. The EDA is characterized by much higher levels of density fluctuations in the barrier region seen by reflectometry[6]. These are broadband, extending to at least 400 kHz usually accompanied by a quasi-coherent feature which can appear anywhere from 60 - 130 kHz. Unlike the  $H\alpha$  signal, which may suggest that the ELM-free to EDA transition is gradual, the fluctuations are seen to turn on abruptly. There is some evidence on the  $H\alpha$  signal of “dithers” between the two regimes. EDA is also accompanied by higher levels of magnetic fluctuations[7,8]. These are also broadband, extending at least to several hundred kHz and without any strong coherent component. The magnetic fluctuations are seen to rotate rapidly in the electron diamagnetic direction, an observation consistent with the presence of a strong negative radial electric field in the plasma edge. Perpendicular rotation speeds are typically in the range 20-60 km/sec implying electric field magnitudes of 100-250 kV/m. This contrasts with spectroscopic observations in the plasma core where  $E_r$  is positive and about a tenth the magnitude.

### 3. EDA and ELM-free H-mode Operational Space

The conditions under which either ELM-free or EDA H-modes are obtained are beginning to be understood. In describing the EDA/ELM-free boundary, it is necessary to define quantitative metrics for sorting discharges into one or the other category. While most H-mode plasmas are clearly classified as one or the other, a certain amount of ambiguity exists in some cases. The  $D_\alpha$  level itself is probably not the best measure, particularly for transient conditions. This is not surprising considering the geometric distribution of this light and its origin as part of both ionization and recombination processes. The presence of high frequency edge fluctuations may be the best indication, but these

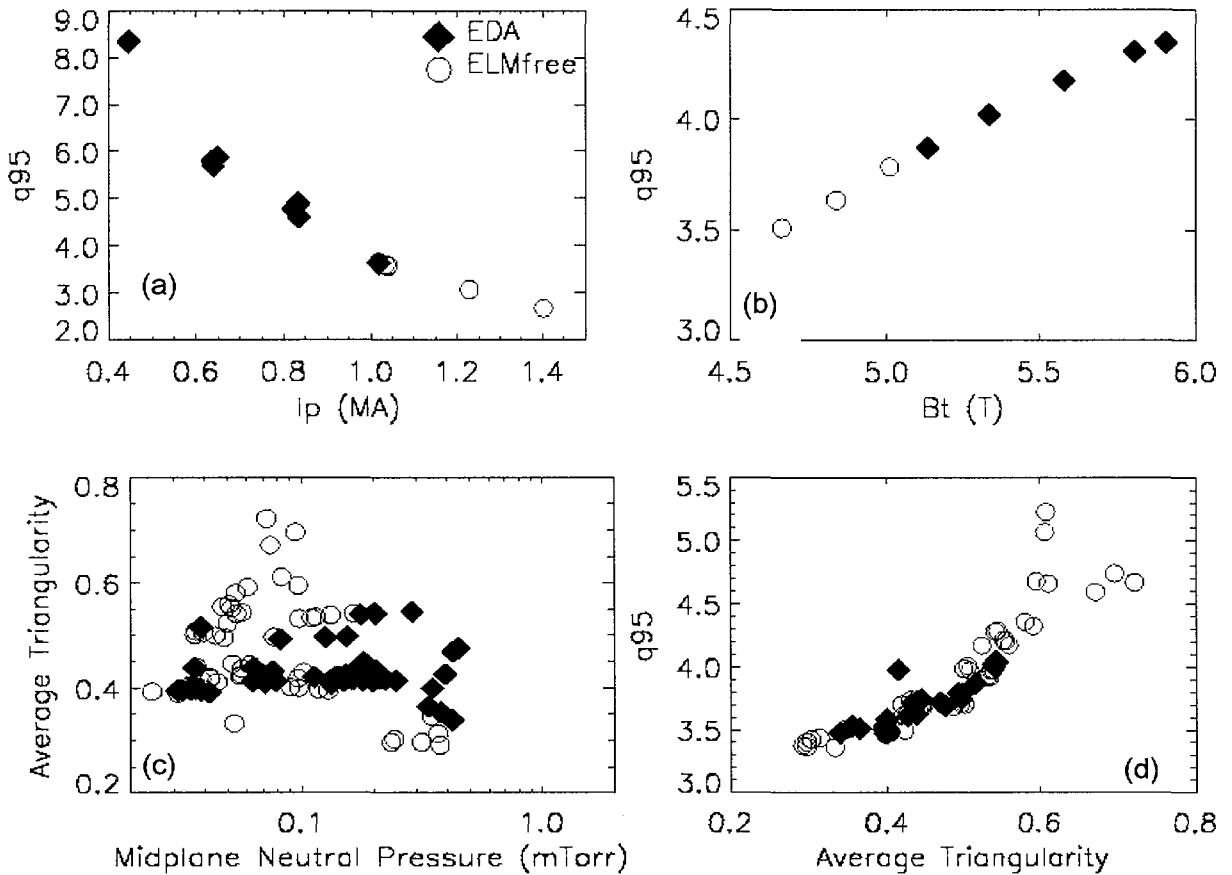


Fig 3. Results of studies to determine EDA-ELM-free boundary. (a). Plasma current scan at 5.3T and standard plasma shape. The transition occurs at about 1 MA or  $q_{95} \sim 3.8$ . (b). A magnetic field scan at  $I_p = 1$  MA and standard shape. Again the transition occurs at  $q_{95} \sim 3.8$ . (c). Occurrence of the two regimes as a function of average triangularity and mid-plane neutral pressure. EDA discharges are seen to occur at moderate values of triangularity and are more likely at higher neutral pressure. (d).  $q_{95}$  plotted for data from the previous graph. In this case ELM-free discharges also occur at the highest values of  $q_{95}$ , suggesting a dependence on both shape and safety factor.

observations are not available for all times or for all discharges. As a practical matter, we have chosen to use impurity accumulation as the final arbiter. Plasmas with impurity radiation steadily increasing with a time constant less than 0.5 seconds (and, of course, with no ELMs) were classified as ELM-free.

EDA plasmas are more likely at the highest target plasma densities and high midplane or divertor neutral pressures. For our standard shape plasmas at 1 MA, discharges with midplane neutral pressures greater than 0.1 mTorr or with ohmic target densities greater than  $1.5\text{-}2 \times 10^{20} \text{ m}^{-3}$  are invariably EDA. EDA is also correlated with high plasma density, but not as strongly as with neutral pressure. High plasma currents favor ELM-free behavior, with a transition near 1 MA, and EDA generally absent at 1.2 MA and above. For the standard shape, and  $B_T = 5.4$  T, 1 MA corresponds to  $q$  at the 95% flux surface,  $q_{95} = 3.7 - 4.0$ . Magnetic field scans at constant current show a transition to EDA as  $q_{95}$  rises to near 4. Figures 3a and 3b summarize the results of current and field scans, where the transition to EDA is seen to occur at approximately the same  $q_{95}$  in either case. Plasma shape also seems to play an important role in determining the type of H-mode. For otherwise identical conditions, discharges with the lowest and highest  $\delta$  were consistently ELM-free while those with moderate  $\delta$  were more likely to be EDA. This can be illustrated in figure 3c where the average triangularity is plotted against midplane neutral pressure. In this plane, regions of predominately EDA and predominately ELM-free can be distinguished. Similar trends can be observed in individual discharges

where  $\delta$  is scanned dynamically. (It must be noted that changes in plasma shape can effect the coupling to the divertor; thus shaping effects cannot be entirely isolated.) The effect of shaping cannot be explained simply as the variation in  $q_{95}$  at constant current. In fact, the trends are opposite to those described above. Figure 3d shows the two regimes in the  $\delta, q_{95}$  plane. In this case, discharges at higher  $q$  are ELM-free. Thus we must conclude that the EDA/ELM-free boundary depends on both  $q_{95}$  and shape.

Edge density profiles measured by reflectometry and electron temperature profiles by ECE show widths which can be less than 1 cm, near the limit of the diagnostic resolution[9]. The temperature width does not show any clear trends with those parameters identified as essential for the EDA/ELM-free boundary and  $\nabla T_e$  is found to be roughly constant under a wide range of conditions. By contrast, an edge soft x-ray array shows the steepest pedestal, with widths as short as 2 mm in high current ELM-free H-modes[10]. Soft x-ray widths also show an inverse dependence on plasma current and a positive correlation with triangularity. Parameters which cause the x-ray width to drop are generally the same as those which cause transitions from EDA to ELM-free behavior. Temperature pedestal heights show relatively little dependence on the type of H mode, which may suggest that the EDA regime mainly affects particle and/or impurity confinement. This would be consistent with the observed weak effect on global energy confinement.

#### 4. Rotation Observations and Scaling

A surprising result from recent C-Mod experiments has been the observation of substantial toroidal rotation in the plasma core in plasmas with ICRF and ohmic heating only[11]. Main ion mach numbers up to 0.3 have been inferred from measurements of impurity rotation, density and temperature. On most other tokamaks, observations of rotation have been made in plasmas with an external momentum source, usually provided by neutral beams.  $E_r$  has been inferred from measured impurity rotation and the force balance equation; a recent comprehensive review may be found in reference [12]. Toroidal impurity rotation in ohmic plasmas (no net momentum input) is consistent with neoclassical predictions [13,14]; in ohmic L-mode discharges, impurities rotate in the direction opposite to the plasma current. It is difficult to separate the contribution to the rotation from the direct momentum input of the neutral beams and the rotation that may be associated with (or induced by) H-modes. ICRF-only heated discharges provide an opportunity for the study of toroidal rotation in auxiliary-heated plasmas with no direct momentum input. Co-current rotation in ICRF-only plasmas [12,15] has been documented, alternately explained by high energy ion loss and the effects of the ion pressure gradient [15].

Measurements in C-Mod were made with a set of von Hamos type crystal x-ray spectrometers. Five of these spectrometers view the plasma at an angle only  $6^\circ$  off perpendicular and are thus more sensitive to poloidal rather than toroidal rotation. Spectrometers view from both positive and negative poloidal and toroidal angles, yielding, in principle, unambiguous measurements of both velocity components. A sixth spectrometer has a tangential view of the plasma core and can make accurate measurements at lower values of toroidal velocity. This instrument is also used to check the accuracy of the larger array. X-ray spectra of the Lyman  $\alpha$  doublet of  $Ar^{17+}$  were recorded and line shapes analyzed to provide measurements of Ar ion temperature, density, and rotation velocity. The force balance equation can then be used to calculate the radial electric field.

In Alcator C-Mod during the ICRF pulse, the rotation is in the co-current direction (opposite to that during the ohmic portion of the discharge). When the plasma current direction is reversed, the rotation during ICRF heating also switches, remaining in the co-current direction. The magnitude of the rotation is largest ( $1.3 \times 10^5$  m/s, 200 kRad/s) during the best H-mode discharges. The magnitude of the rotation velocity during ICRF heating increases with the stored energy increase, regardless of input power or electron density, over a range of two orders of magnitude. The plasmas with the highest H-factors rotate the fastest. In general, the rotation is not an effect only of H-mode *per se*;

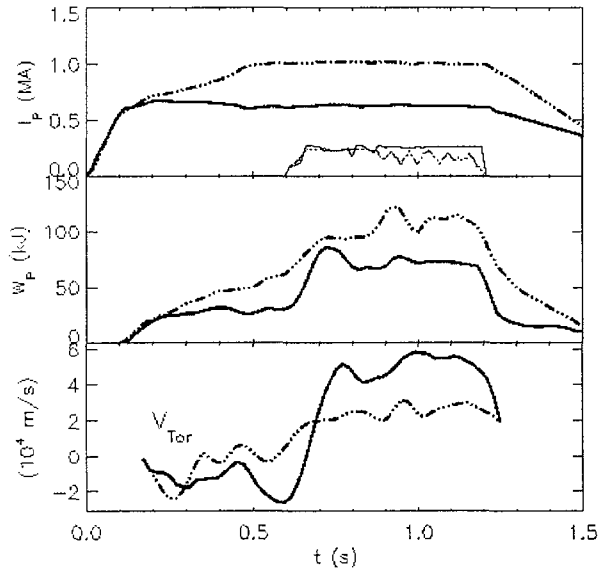


Fig. 4. Time histories of the plasma current and ICRF pulse (top), plasma stored energy (middle) and argon toroidal rotation velocity (bottom) for a 0.6 MA discharge (solid line) and 1.0 MA discharge (dash-dot).

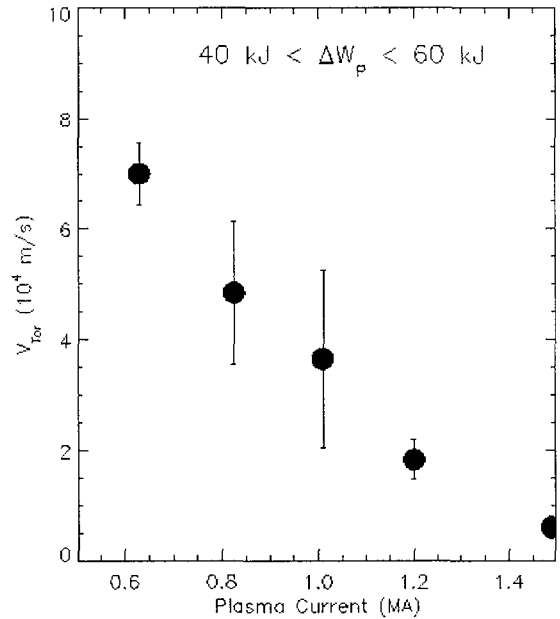


Fig. 5. The central toroidal rotation velocity as a function of plasma current for stored energy increases between 40 and 60 kJ

some high H-factor L-mode plasmas rotate faster than some modest H-factor H-mode plasmas. The toroidal rotation velocity is peaked at the magnetic axis, and falls off quickly with minor radius. Any poloidal component of the rotation velocity inside of 0.06 m is  $< 3 \times 10^3$  m/s. While the trend of increasing rotation velocity with increasing stored energy is clear, there is a certain amount of scatter in the data, some of which is due to dependence on the plasma current. In otherwise similar plasmas with comparable stored energy increases, the toroidal rotation is higher in plasmas with lower current. This effect is demonstrated in figure 4, where the time histories of the plasma current, stored energy and rotation velocity are shown for two 5.4 T discharges with 2.5 MW of ICRF power between .6 and 1.2 s. The stored energy increase during the ICRF pulse in both cases is about 45 kJ, although the 1 MA plasma has a higher stored energy target plasma before .6 s. The 600 kA plasma rotates about a factor of two faster compared to the higher current case. This trend of higher rotation with lower plasma current is emphasized in figure 5, which shows the toroidal rotation velocity as a function of plasma current, for fixed plasma stored energy increase.

The rotation velocity decays with a characteristic time between 50 and 100 ms following the ICRF turn-off, slightly less than the energy confinement time, and much shorter than the predicted neoclassical momentum slowing down time. For argon, the diamagnetic contribution to  $E_r$  from the force balance equation,  $\nabla P / neZ$ , is negligible compared to the rotation terms. Values of  $E_r$  up to 30 kV/m at  $r/a = .3$  have been inferred, although  $V_\theta B_T / B_p$  has been ignored compared to  $V_\phi$ . The inference is that during the ICRF heating, a strong radial electric field forms near the plasma center.

## 5. Rotation - Possible Origin

In an effort to understand this rotation from basic neo-classical considerations, measured central impurity rotation profiles [11] for an ELM-free ICRF H-mode plasma have been compared with the calculated neo-classical impurity rotation profiles, evaluated using the expressions in Ref.[14]. These profiles are shown in figure 6.  $E_r$  is not included in these profiles since there is no independent or direct measurement, and no first-principles calculation. Also shown are the calculated *main ion* profiles. The measured core value for  $V_\theta \leq 3 \times 10^3$  m/s is consistent with the calculations. However, the central impurity toroidal rotation profiles can only be made to agree with the calculations by

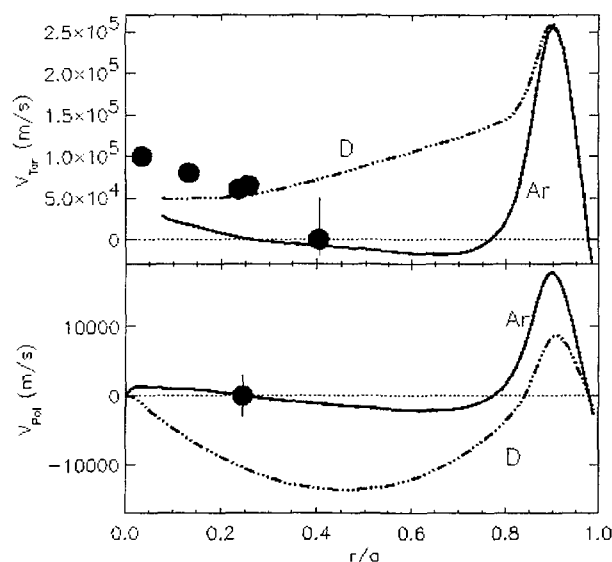


Fig. 6. Calculated toroidal (top) rotation velocity profiles for argon ions (solid) and deuterons (dash-dot-dot-dot) and poloidal rotation velocity profiles (bottom) for an ELM-free ICRF H-mode discharge. The filled circles show the measured argon toroidal and poloidal rotation velocities

inclusion of a substantial core  $E_r$ . The suggestion is that, during the ICRF H-mode, there is the formation of a strong radial electric field near the plasma center which leads to the central toroidal rotation.

One possible mechanism that can give rise to  $E_r$  is an inward shift of energetic ion orbits induced by ICRF waves [16]. During H minority heating at 5.4 T with an ICRF at 80 MHz and  $n_H/n_D=2-5\%$ , an ion tail is formed, with energies in the 20-50 keV range. These ions interact with the RF at resonance locations given by  $\omega = \omega_{ci} - k_{\parallel}v_{\parallel}$ . For C-Mod,  $k_{\parallel} \approx 15m^{-1}$ , leading to a resonance shift of  $1 - 2 \times 10^7 s^{-1}$ , which corresponds to a displacement of several cm in the resonance location. This displacement, combined with the neo-classical orbit shift, allows certain classes of fast particles to interact more strongly with the RF fields, breaking the  $k_{\parallel}$  symmetry and leading to net ion flows. For our parameters, the net movement is inward and this small non-ambipolar flow can create a substantial positive  $E_r$ . The toroidal rotation is the plasma's response to this imposed field. In addition to the correct sign of the rotation, this theory also predicts the approximate magnitude of the induced rotation and its observed current dependence.

## 6. Discussion

EDA seems to be a regime where the edge pedestal gradients are relaxed by a continuous rather than an intermittent process. Even when small ELMs are seen on top of the EDA as shown in figure 2, these do not seem to carry out any measurable amount of energy or particles, nor do they diminish the size of the pedestal. By contrast, type I ELMs are believed to be a relaxation oscillation driven by the improved transport in the H-mode barrier and limited by pressure driven [17] or current driven [18] MHD modes. Hegna [19] and Connor [20] have formulated a picture for ELM behavior by calculating stability in the  $J_a, \alpha$  plane (where  $J_a$  is the edge current density and  $\alpha$  is the normalized edge pressure gradient,  $R\beta'$ ). In this picture, the edge of an H-mode plasma evolves to the pressure driven ballooning limit on a transport time scale, then toward the current driven "peeling mode" limit on a current diffusion time scale. The ballooning limit is seen as a "soft" limit, where transport is increased but the pedestal remains intact. ELMs are identified with the peeling limit, which is essentially an external kink, and results in destruction of the barrier. We note that one might expect to see an increase in edge turbulence as an ELM-free discharge approaches its first large ELM; in fact this is not generally observed. The observed dependence on triangularity and safety factor suggest that MHD stability also plays an important role in determining the EDA/ELM-free boundary. Superficially, the dependences are reminiscent of those reported by Miller [21], where the plasma edge was shown to have the easiest access to second stability at moderate  $\delta$  and at higher  $q_95$ . However, to

make that connection, we would have to identify EDA as the more MHD stable regime. This view is contradicted by the increased level of turbulence and decreased particle confinement seen in EDA.

The MHD topology is rather complicated however, depending critically on the local magnitude of edge current density and pressure gradient. Thus individual flux surfaces within the pedestal may be near one of several stability limits. The effects of shaping and safety factor discussed above cannot be explained by a simple  $S/q^2$  analysis. Resolution of these issues must await improved measurements of these profiles planned for future experimental campaigns. The observed effects of neutrals may ultimately be explained within the same model. We note that high levels of neutrals in the plasma edge can lower the edge temperature through direct cooling (via charge exchange and convective losses) or by weakening the transport barrier via shear flow damping. We have observed slower mode rotation at high neutral densities, which can be interpreted as damping of the underlying perpendicular flows[8]. Regardless of the mechanism, lower edge temperatures are observed at high neutral densities from which we can infer higher collisionalities and smaller edge currents from both the ohmic and bootstrap drives. These effects will tend to keep the plasma edge away from the peeling boundary and thus suppress type I ELMs. Finally we note the possible connection to theories of drift Alfvén turbulence. Three dimensional electromagnetic simulations show that plasmas at higher collisionality are subject to turbulence due to the non-linear evolution of resistive ballooning modes [22].

The observation of strong rotation driven in ICRF heated plasmas suggests the possibility of creating and controlling internal transport barriers (ITB) with minority heating ICRF alone. The standard model for formation of ITBs relies on turbulence suppression by sheared ExB flows. The seed for these flows is believed, in many cases, to be from beam driven rotation. In a reactor, with its large value of  $n_{e,a}$ , it is unlikely that neutral beams can be used to drive significant rotation. RF drives may provide a substitute, but creating such a barrier would require more rotation than has been observed so far. It should be possible to increase the drive by increasing the input power and by launching an asymmetric  $k$  spectrum[16]. Of course, RF alone will not provide an internal particle source, which may be a critical component for ITB formation.

## References

- [1] Snipes, J.A. , et al., Proc. 24th EPS Conference, Berchtesgaden, Vol. 21A, Part II (1997) 565.
- [2] Greenwald, M., et al., Nuclear Fusion, **37** (1997) 793.
- [3] Bures, M., et al., Nuclear Fusion, **32** (1992) 539.
- [4] Ozeki, T., et al., Nuclear Fusion, **30** (1990) 1425.
- [5] Kamada, Y., et al., Plasma Physics and Controlled Fusion **38** (1996) 1387.
- [6] Stek, P., "Reflectometry Measurements on Alcator C-Mod", PhD. Thesis (1997).
- [7] Snipes, J.A. et al., Plasma Physics and Controlled Fusion, **40** (1998) 765.
- [8] Hutchinson, I.H., et al., "Edge Transport Barrier Phenomena in Alcator C-Mod, to be published in Plasma Physics and Controlled Fusion.
- [9] Hubbard, A.E., et al., Physics of Plasmas **5** (1998) 1744.
- [10] Granetz, R., Osborne, T., et al., these Proceedings.
- [11] J. E. Rice et al., Nucl. Fusion **38** (1998) 75.
- [12] K. Ida et al., Plasma Physics and Controlled Fusion **40** (1998) 1429.
- [13] J.E. Rice et al., Nucl. Fusion **37** (1997) 421.
- [14] Y.B. Kim, P.H. Diamond and R.J. Groebner, Phys. Fluids B **3** (1991) 2050.
- [15] L.-G. Eriksson et al., Plasma Phys. Contr. Fusion **39** (1997) 27.
- [16] C. S. Chang. et al., these Proceedings.
- [17] Gohil, P. et al., Physical Review Letters **61** (1988) 1603.
- [18] Manickam, J., Phys. Fluids, B **4**, (1992) 1901.
- [19] Hegna, C., et al., Phys. Plasmas **3**, (1996) 248.
- [20] Connor, J.W. and Wilson, H.R., "Theory of Fusion Plasmas", edited by Connor, Sindoni, and Vaclavik, (Bologna: Editrice Compositiori), 441
- [21] Miller, R.L., et al., Physics of Plasmas **4** (1996) 1062.
- [22] Rogers, B.N. and Drake, J.F., Physical Review Letters **79** (1997) 229.